Journal of Materials Science: Materials in Medicine (2018)29:75
https://doi.org/10.1007/s10856-018-6056-2

BIOMATERIALS SYNTHESIS AND CHARACTERIZATION

Original Research

Carbodiimide cross-linking counteracts the detrimental effects of gamma irradiation on the physical properties of collagen-hyaluronan sponges

Jay M. Patel[1,2] · Ryan C. Jackson[1] · Greta L. Schneider[1] · Salim A. Ghodbane[1,2] · Michael G. Dunn[1,2]

Received: 1 September 2017 / Accepted: 4 April 2018
© Springer Science+Business Media, LLC, part of Springer Nature 2018

Abstract

Collagen-based scaffolds are extensively used in biomaterials and tissue engineering applications. These scaffolds have shown great biocompatibility and versatility, but their relatively low mechanical properties may limit use in orthopaedic load-bearing applications. Moreover, terminal sterilization with gamma irradiation, as is commonly performed with commercial devices, presents concerns over structural integrity and enzymatic stability. Therefore, the goal of this study was to test the hypothesis that EDC/NHS cross-linking (10 mM/5 mM) can protect collagen-hyaluronan sponges from the damaging effects of gamma irradiation. Specifically, we evaluated compressive and tensile mechanical properties, enzymatic stability, porosity and pore size, and swelling ratio. Ultimate tensile strength and elastic modulus exhibited increases (168.5 and 245.8%, respectively) following irradiation, and exhibited over tenfold increases (1049.2 and 1270.6%, respectively) following cross-linking. Irradiation affected pore size (38.4% decrease), but cross-linking prior to irradiation resulted in only a 17.8% decrease. Cross-linking also showed an offsetting effect on the equilibrium modulus, enzymatic stability, and swelling ratio of sponges. These results suggest that carbodiimide cross-linking of collagen-hyaluronan sponges can mitigate the structural damage typically experienced during gamma irradiation, warranting their use in tissue engineering applications.

Graphical Abstract

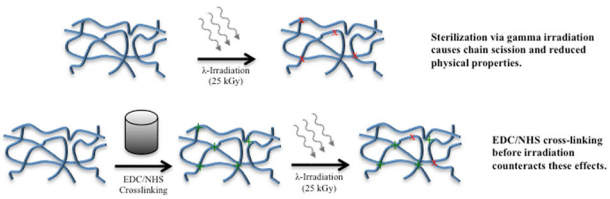

1 Introduction

Collagen is one of the most widely used biomaterials for tissue engineering and regenerative medicine. It can be fabricated into sponges, hydrogels, films, powders, and tubes, allowing for a wide range of biomaterials applications [1–6]. The porous microstructure of collagen sponges enables cellular infiltration and matrix remodeling [7, 8]. The addition of proteoglycans or glycosaminoglycans [9, 10], such as hyaluronan [11–13], can enhance both scaffold mechanics and cellular activities, such as migration, proliferation, and even differentiation. While these materials have demonstrated strong biological potential in

✉ Jay M. Patel
jaymilanpatel@gmail.com

✉ Michael G. Dunn
dunnmg@rwjms.rutgers.edu

[1] Department of Orthopaedic Surgery, Rutgers Biomedical and Health Sciences–Robert Wood Johnson Medical School, 1 Robert Wood Johnson Place, MEB 424, New Brunswick, NJ 08901, USA

[2] Department of Biomedical Engineering, Rutgers–The State University of New Jersey, 599 Taylor Road, Piscataway, NJ 08854, USA

Published online: 28 May 2018

musculoskeletal applications [1, 2, 14, 15], their relatively low mechanical properties limit their use in functional in vivo models [16]. Moreover, terminal sterilization with gamma irradiation during product manufacturing can further affect the physical properties of these biomaterials, through either the direct scission of alpha polypeptides or the presence of free radicals [17, 18]. Improving the properties of collagenous implants, including protection from sterilization effects, is required for use in any load-bearing applications.

Cross-linking of these biological sponges provides a method of improving the mechanical properties by facilitating bonding between collagen molecules [19, 20]. Intermolecular crosslinking can strengthen collagen scaffolds by preventing the sliding of individual collagen fibers, and can improve enzymatic stability. Various chemical cross-linkers have been used for collagen, including glutaraldehyde [21, 22], carbodiimide [19, 21, 23], and diamines [23]. Glutaraldehyde offers short crosslinking times and increased resistance to degradation, but has also shown cytotoxic effects on cells [5, 21, 24]. This cytotoxic effect reduces cellular growth in vitro and in vivo due to the presence of unreacted functional groups or by release of those groups during enzymatic degradation of cross-linked biomaterial.

Carbodiimide, mostly 1-ethyl-3-(3-dimethylaminopropyl) carbodiimide (EDC), has been used more frequently due to lower cytotoxicity concerns [21]. It increases the mechanical strength and enzymatic stability of collagen scaffolds, and cross-linking concentrations can be adjusted to achieve desired mechanics and porosity [19, 25]. EDC-crosslinking has previously been shown to provide radioprotection of tendon allografts [26]; however, the combinatorial effects of gamma sterilization and EDC-crosslinking on the physical properties of biological sponges have yet to be fully characterized [20]. We hypothesized that EDC crosslinking of collagen-hyaluronan sponges could counteract the harmful effects of gamma irradiation on mechanical, enzymatic, and structural properties.

2 Methods

In this study, four different groups of collagen-hyaluronan sponges were fabricated: Control (untreated), Irradiated (IR), Cross-linked (XL), and Cross-linked Irradiated (XL + IR). The sponges were evaluated mechanically with confined compression and ultimate tensile testing. Enzymatic stability was tested with a bacterial collagenase degradation assay. Structural properties were evaluated by measuring swelling ratio, pore size, and porosity.

2.1 Sponge preparation

The sponge preparation was adapted from a previous study [4]. Bovine Achilles tendon collagen (Worthington Biochemical Corporation, Lakewood NJ) was ground into a powder with particle size < 425 µm. Sodium hyaluronate (Acros Organics, Thermo Fisher Scientific, Waltham MA) was dissolved (0.25 g/L) in dilute hydrochloric acid (HCl, pH 2.35). Collagen was swollen in the acid solution (20 g/L) to form a 2% w/v dispersion, degassed under vacuum, and poured into petri dishes approximately 6 mm in thickness. The dispersion was frozen via ethanol-dry ice bath for 20 min, and lyophilized at −50 °C and 0.06 mbar (FreeZone 1, Labconco, Kansas City MO) for 24 h. Collagen-hyaluronan sponges were utilized due to their common use in biomaterials applications [12, 13].

Sponges in the XL and XL + IR groups were cross-linked in solution containing 10 mM EDC and 5 mM N-hydroxysuccinimide (NHS) for 6 h (200 mL solution/1 g collagen). Sponges were subjected to three 10-minute rinses in DI H_2O, one 2-h rinse in 100 mM sodium phosphate (Na_2HPO_4), and one 24-h DI H_2O rinse. Sponges were frozen again via ethanol-dry ice bath and lyophilized. Sponges in the IR and XL + IR groups were gamma irradiated at 25 kGy (Sterigenics, Rockaway NJ) at room temperature.

2.2 Confined compression

Samples were tested in confined compressive creep, as is commonly done with musculoskeletal load-bearing tissues [27, 28]. From sponges in all groups, 4 mm-diameter plugs were excised using a biopsy punch ($n = 10$ per group). Each plug was hydrated in phosphate buffered saline (PBS) for at least 30 min and loaded into a custom 4 mm-chamber with a unidirectional metal fluid flow filter (Fig 1a). Each sample was preloaded to 0.05 N, and loaded at 0.5 N compression for 3600 s using a uniaxial mechanical testing machine

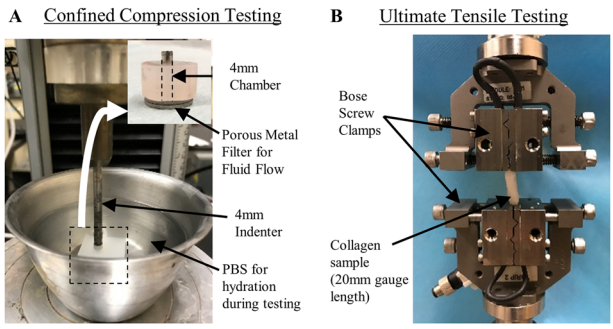

Fig. 1 **a** Confined compression testing apparatus with 4 mm indenter, 4 mm chamber with porous metal filter for unidirectional fluid flow. **b** Ultimate tensile testing apparatus using Bose screw clamps

(Instron #5542, Instron Corporation, Norwood MA). The equilibrium modulus was calculated based on equilibrium stress ($0.5\ N/4\pi mm^2 = 0.040\ MPa$), displacement, and initial height at preloading.

2.3 Swelling ratio and ultimate tensile testing

Tensile testing samples (width: 5 ± 1 mm, length: ≥40 mm) were excised from sponges. Sample dimensions were measured in three locations along its length to determine average width and thickness using a laser micrometer (Model 1202B, Z-Mike, Dayton OH). The samples were weighed before and after hydration in PBS. The swelling ratio was calculated as the mass of the hydrated sponge divided by that of the dry sponge. After hydration, samples were loaded into screw clamps (Bose, Eden Prairie MN) with a gauge length of 20 mm (Fig. 1b), and strained at a rate of 5 mm/min to failure. Samples that slipped from or broke within the clamps were omitted and replaced to obtain $n = 9$ per group. From the load-displacement curve and measured dimensions, ultimate tensile strength (UTS) and elastic modulus (EM) were calculated in MATLAB.

2.4 Enzymatic stability

Enzymatic stability was tested with an in vitro collagenase resistance test. Collagen samples were cut to a mass of 2.0 ± 0.3 mg ($n = 9$ per group). Samples were incubated to 37 °C in 1 × Tris buffer (0.5 mL/1 mg sponge) before testing. Following incubation, a 500 U/mL bacterial collagenase solution (*Clostridium histolyticum*, Sigma-Aldrich, St. Louis MO) was added to each sample (0.5 mL/1 mg sponge), giving a final 250 U/mL solution. Samples were incubated at 37 °C and assessed visually every 10 min with a semi-quantitative scale from 0 to 5, with 0 representing total dissolution and 5 representing a fully-intact sample. Samples were randomized and graded blindly. The enzymatic degradation profile and time to dissolution were obtained.

2.5 Pore size via scanning electron microscopy (SEM)

Sponges from all four groups were sectioned to obtain pore structure from an interior surface to eliminate any edge effects during fabrication. Samples were sputter coated in gold and imaged at 100× magnification on a field emission SEM (Carl Zeiss Microscopy, Thornwood NY) at the Department of Materials Science and Engineering (Rutgers University, Piscataway NJ). Thirteen images from each group were converted to binary by applying an adaptive thresholding algorithm. The major and minor axis of each ellipsoidal pore were calculated using a custom MATLAB script, and the axes were multiplied by a factor of 1.5 to account for sectioning angles that did not encompass the maximal cross-section of each pore [29, 30]. The resultant major and minor axes were averaged to obtain a mean intercept length, which was averaged for each image to obtain an average pore size.

2.6 Porosity

Porosity was determined using an ethanol infiltration assay. Four-mm diameter biopsy punches were excised from sponges ($n = 9$ per group). Plugs were dried under vacuum, weighed (m_{dry}), and measured for height using Vernier calipers. Then, plugs were submerged in 100% ethanol for 60 min under gentle agitation. Wet plugs were superficially dried and weighed (m_{wet}). Pore volume was found by subtracting the dry weight from wet weight, and dividing by the density of ethanol ($\rho_{ethanol} = 0.789$ g/mL). Porosity (ϕ_{sponge}) was then calculated (Eq. 1) by dividing the pore volume by the total volume ($V = \pi r^2 h$).

$$\Phi_{sponge} = (m_{wet} - m_{dry})/(\rho_{ethanol} * \pi r^2 h) \quad (1)$$

2.7 Statistical analysis

The equilibrium compressive modulus, ultimate tensile strength, elastic tensile modulus, swelling ratio, time to dissolution, and porosity of the four groups were compared using a two-way analysis of variance ($p < 0.05$) to measure the effects of cross-linking, irradiation, and their interactions. A post-hoc Bonferroni correction ($p < 0.05$) was used to determine statistical differences between groups. Pore size was compared using a two-way Friedman's test ($p < 0.05$) due to a non-normal distribution. All statistical analyses were performed in Stata 14 statistical software (StataCorp, College Station TX).

3 Results

3.1 Sponge preparation

At least two sponges (1 g each) were fabricated per group. For each test, samples were taken from all sponges within each group. No observable or statistical differences occurred between sponges of the same group. Any variability in sponge height was accounted for in the assays by using material properties.

3.2 Confined compression

Equilibrium modulus was significantly influenced by crosslinking ($p = 0.0192$) but not by irradiation ($p =$

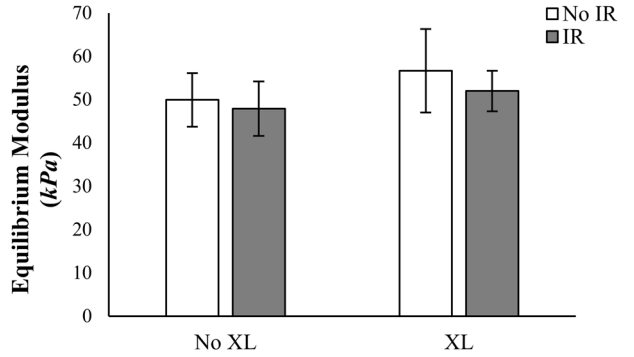

Fig. 2 Equilibrium modulus of the four groups with No IR or IR, and No XL or XL ($n = 10$ per group). IR = irradiation, XL = cross-link. Mean ± standard deviation

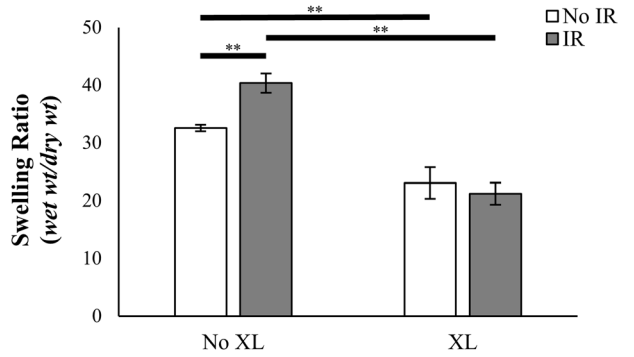

Fig. 3 Swelling ratio (wet weight/dry weight) of all sponges ($n = 9$ per group). IR = irradiation, XL = cross-link. Mean ± standard deviation. * denotes statistically significant difference ($p < 0.05$), ** denotes highly statistically significant difference ($p < 0.001$)

0.1382). XL sponges (56.62 ± 9.64 kPa) exhibited a modulus 13.4% greater than control sponges (49.91 ± 6.20 kPa). Irradiation of control sponges led to only a 4.05% decrease in equilibrium modulus, with XL + IR sponges showing a similar decrease from XL sponges (Fig. 2).

3.3 Swelling ratio and ultimate tensile testing

Both crosslinking and irradiation had a highly significant influence on swelling ratio ($p < 0.001$). IR sponges (40.36 ± 1.67) experienced more swelling than control sponges (32.55 ± 0.58). However, irradiation did not alter the swelling ratio of cross-linked sponges ($p = 0.257$), with both cross-linked groups experiencing significant decreases in swelling ratio from their respective non-cross-linked group (Fig. 3).

Irradiation had a positive influence ($p < 0.05$) on ultimate tensile strength (1.68-fold increase) and elastic modulus (2.46-fold increase). Cross-linked sponges exhibited a 10.49 and 12.71-fold increase over control sponges in ultimate tensile strength and elastic modulus, respectively ($p < 0.001$). Irradiating the cross-linked sponges provided an

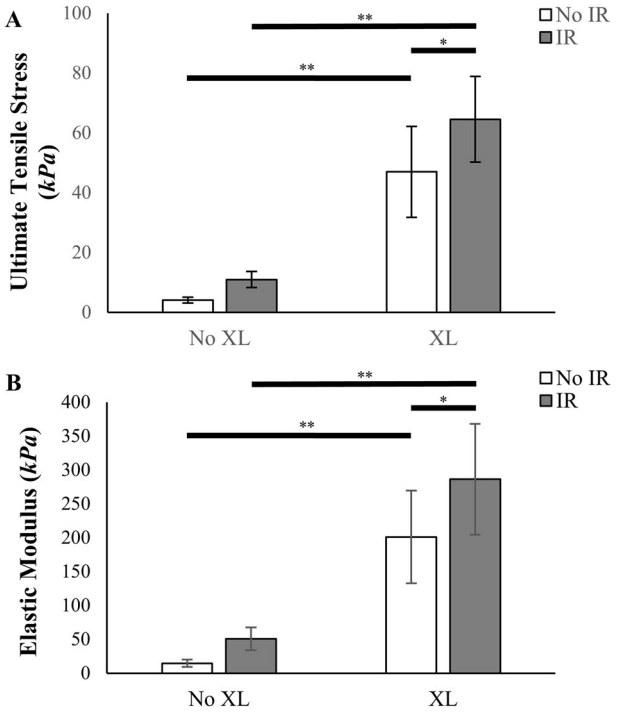

Fig. 4 Ultimate tensile properties of all sponges ($n = 9$ per group). **a** Ultimate tensile strength and **b** elastic modulus. IR = irradiation, XL = cross-link. Mean ± standard deviation. * denotes statistically significant difference ($p < 0.05$). ** denotes highly statistically significant difference ($p < 0.001$)

additional 37.3 and 42.3% increase in each parameter. Overall, the XL + IR sponges (UTS: 286.2 ± 82.0 kPa, EM: 64.5 ± 14.3 kPa) displayed a highly significant improvement over control sponges (UTS: 14.7 ± 5.3 kPa, EM: 4.09 ± 0.97 kPa), showing additive effects from cross-linking and irradiation (Fig. 4).

3.4 Enzymatic stability

The enzymatic degradation profile of sponges showed effects of cross-linking and irradiation (Fig. 5). Control sponges experienced complete dissolution in 92 ± 13 min; IR sponges (81 ± 3 min) displayed a more rapid dissolution profile (Fig 5a). Cross-linking drastically elongated ($p < 0.001$) the dissolution of sponges, both in terms of the overall profile and with regards to the time to dissolution (173 ± 18 min). The XL + IR group experienced a profile between that of control and XL sponges, with a dissolution time of 137 ± 22 min.

3.5 Pore size via SEM

Crosslinking had a minimal effect on pore size ($p = 0.1362$), with only a 0.95% decrease from control to XL sponges. However, irradiation significantly reduced pore size ($p = 0.0099$), with IR sponges having an average pore

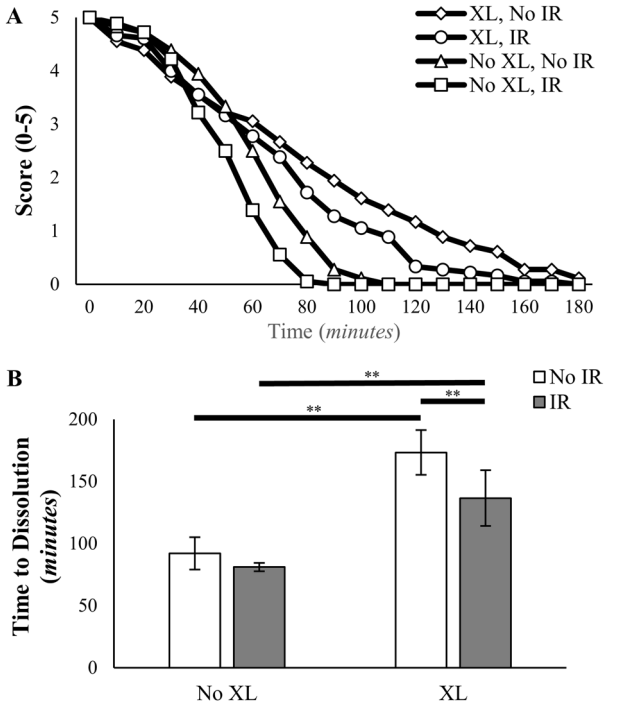

Fig. 5 Enzymatic stability results. **a** Dissolution profile measured every 10 min, and **b** Time to dissolution (minutes) for sponges from all groups ($n = 9$ per group). IR = irradiation, XL = cross-link. Mean ± standard deviation. ** denotes highly statistically significant difference ($p < 0.001$)

size 38.4% lower than control sponges. On the other hand, XL + IR sponges only experienced a 17.8% decrease from their XL counterparts. Characteristic SEM images and the resulting pore sizes are shown in Figs. 6a, b.

3.6 Porosity

Porosity was highly significantly decreased by cross-linking ($p < 0.001$), with no statistical influence by irradiation ($p = 0.062$). The XL + IR group (85.83 ± 5.83%) had a porosity that was 3.98% lower ($p = 0.374$) than that of the XL group (89.39 ± 3.34%). Both non-cross-linked groups (control, IR) had porosities greater than 95%. Porosities are shown in Fig 6c.

4 Discussion

Collagen-based scaffolds have been developed for a variety of load-bearing applications, including total meniscus reconstruction [31], ACL regeneration [32], and articular cartilage repair [33]. Collagen sponge-like scaffolds have demonstrated great potential and versatility; the sponges in this study were made in Petri dishes, but the collagen-hyaluronan dispersion could be injected into a variety of shapes and sizes. Regardless of the application, terminal

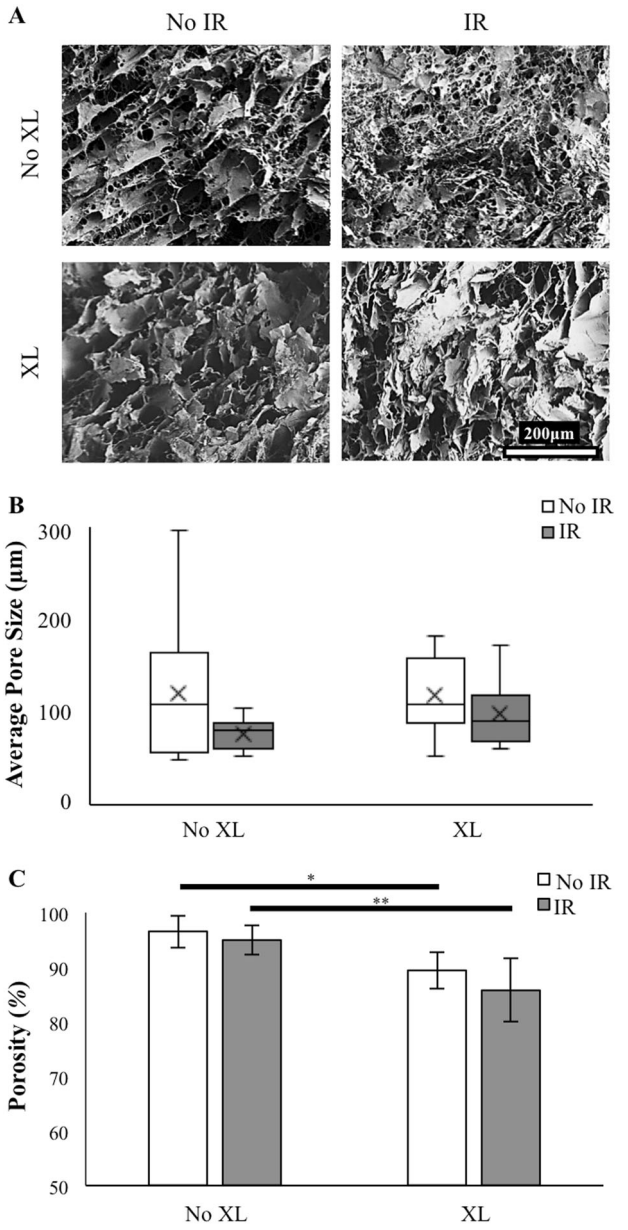

Fig. 6 **a** Representative scanning electron micrographs of sponges from all four groups. Scale bar represents 200 µm. **b** Average pore size (µm) of all groups ($n = 13$ per group) as box-and-whisker plot. Whiskers represent minimum and maximum, box represents 25 and 75th percentile, X represents mean, horizontal line represents median. **c** Porosity (%) of all groups ($n = 9$ per group). IR = irradiation, XL = cross-link, Mean ± standard deviation. * denotes statistically significant difference ($p < 0.05$). ** denotes highly statistically significant difference ($p < 0.001$)

sterilization is often required to guarantee scaffold safety. Gamma irradiation has been shown to provide sufficient sterilization by damaging nucleic acids and structural proteins, via direct chain scission and free radical generation. While these two mechanisms effectively kill bacteria and viruses within constructs, they also result in physical changes to collagen macromolecules [17]. Previously,

Seto et al. showed that irradiation decreased the tensile mechanics of rabbit Achilles tendon allografts, but that cross-linking could potentially compensate for radiation damage [26]. The results of this study showed gamma irradiation actually improved tensile mechanics, but also that cross-linking prior to irradiation could counteract radiation effects on compressive mechanics, enzymatic stability, and pore size.

The mechanical properties of collagen or ECM-derived sponges are integral to their function, especially in load-bearing applications. In compression, the control collagen-hyaluronan sponges displayed an equilibrium modulus of 49.9 ± 6.2 kPa, comparable to previously established steady-state values [17]. Cross-linking and irradiation had minimal effect on the equilibrium modulus, with cross-linking counteracting the slight decrease caused by irradiation. On the other hand, tensile properties of sponges were significantly improved by both cross-linking and irradiation. The mechanical benefits of EDC-crosslinking were expected, with greater than 10-fold increases in tensile properties, consistent with the literature [19, 21, 34]. Irradiation also improved tensile properties of collagen sponges, but to a lesser extent than crosslinking (i.e., 246% increase in elastic modulus). Mazor et al. found a similar (250%) increase in modulus with irradiation of a collagenous wound dressing [35], attributing the increase to crosslinks that form during irradiation. The differences in mechanical outcomes with regards to compression and tension likely result from the ability of these newly formed crosslinks to resist being pulled apart, but inability to keep pores from collapsing during compression.

Previous studies have shown that gamma irradiation decreases the tensile mechanics of tendon allografts [26, 36]. The differences between the response of sponges and tendon allografts to irradiation can be attributed to the differences in cross-linking density prior to sterilization. During irradiation, biological materials experience both degradation and cross-link formation. Tendon is already a highly cross-linked tissue, meaning relatively few cross-links are added during irradiation, and that considerably more degradation occurs. On the other hand, the collagen sponges are substantially less cross-linked than tendons, resulting in significantly more cross-linking than degradation, and ultimately an increase in tensile properties [37]. Thus, mechanically, cross-linking of sponges was able to counteract the effects of irradiation on compressive properties, and further build upon the tensile improvements.

The effects of chain scission and formation of additional cross-links during irradiation were also observed with regards to sponge porosity. The control sponges in this study displayed pore size [38] and porosity [21, 39] consistent with the literature. The chain scission and cross-link formation during irradiation likely caused the large porous structures to break apart and form smaller pores [18], explaining the significant reduction in pore size in irradiated sponges. EDC cross-linking prior to irradiation diminished these changes, providing some mediation to the effects of irradiation. Other studies have shown that EDC or glutaraldehyde cross-linking can in fact increase pore size [34, 39], due to the development of a more organized lattice structure. In this study, cross-linking did reduce the porosity of scaffolds, likely due to this more-organized structure. The reduction in porosity also explains the lower swelling ratio in cross-linked groups, both due to more empty space within the sponges and due to less binding sites for water. With a porosity above 85% and average pore size of near 100 μ, the XL + IR sponges can still allow for adequate cellular infiltration and tissue remodeling.

In addition to offsetting or even improving the mechanical and structural properties described, another integral parameter was enzymatic stability. As anticipated [18], gamma irradiation decreased the enzymatic stability of the collagen sponges in this study, indicating that while cross-links form during irradiation, the overall cleavage of peptide bonds leaves the sponges more susceptible to degradation. On the other hand, EDC cross-linking has been shown to stabilize the enzymatic degradation profile [7, 34], almost doubling time to dissolution in this study. XL + IR sponges exhibited a degradation profile and time to dissolution approximately halfway between control and XL sponges, indicating that EDC cross-linking provides a degree of stability through irradiation by either reducing peptide cleavage during irradiation or by simply providing additional crosslinks.

This study was not without its limitations. First, sponges were fabricated in Petri dishes, allowing for potential edge effects with regards to freezing rates and lyophilization. In order to minimize this effect, we took samples from different sponges from the same relative location. Additionally, even though all sponges were frozen via ethanol-dry ice bath, freezing rates and the resulting porosity of the sponges may have exhibited some variability.

Lastly, this study did not investigate molecular or biological properties, in order to place an emphasis on the biomaterial's physical properties. Previous studies have shown that FTIR of EDC-cross-linked collagen sponges have shown a decrease in the amide II band, indicating a reduction in free NH_2 groups during cross-linking [21]. However, these molecular changes were not as drastic as those observed during glutaraldehyde cross-linking. Moreover, gamma irradiation has also shown a decrease in the amide II band, likely due to decay of the amide groups [40]. With regards to cellular properties, EDC-crosslinking has shown maintenance of cell viability [34], especially compared to glutaraldehyde crosslinking [21]. However, gamma irradiation has shown dose-dependent detrimental effects to

cellular properties of these biomaterials [18, 40]. Future studies should aim to characterize the combinatorial effects of cross-linking and irradiation on the chemistry and biology of the sponges.

Overall, this study showed that EDC-crosslinking provided substantial improvements to the physical properties of collagen-hyaluronan sponges, especially with regards to offsetting the damage caused by gamma irradiation. Crosslinking specifically counteracted the damaging effects of irradiation on equilibrium modulus, swelling ratio, enzymatic stability, and pore size. The results of this study warrant the use of cross-linked, gamma-sterilized biological sponges for tissue engineering applications.

Acknowledgements The authors thank the Orthopaedic Research Laboratory at Rutgers Biomedical and Health Sciences for their assistance in completing this study. They also thank Sukanya Murali for performing the SEM processing and imaging. This study was funded, in part, by the Department of Orthopaedic Surgery discretionary fund.

Compliance with ethical standards

Conflict of interest J.M.P. serves as a consultant for NovoPedics, Inc. M.G.D serves as interim secretary and treasurer and owns stock inNovoPedics Inc. The remaining authors declare that they have no conflict of interest.

References

1. Merriam AR, Patel JM, Culp BM, Gatt Jr. CJ, Dunn MG. Successful total meniscus reconstruction using a novel fiber-reinforced scaffold: a 16 and 32-week study in an ovine model. Am J Sports Med. 2015;43:2528–37. https://doi.org/10.1177/0363546515595065.
2. Geiger M, Li RH, Friess W. Collagen sponges for bone regeneration with rhBMP-2. Adv Drug Deliv Rev. 2003;55:1613–29.
3. Glowacki J, Mizuno S. Collagen scaffolds for tissue engineering. Biopolymers. 2008;89:338–44. https://doi.org/10.1002/bip.20871.
4. Ghodbane SA, Dunn MG. Physical and mechanical properties of cross-linked type I collagen scaffolds derived from bovine, porcine, and ovine tendons. J Biomed Mater Res A. 2016;104:2685–92. https://doi.org/10.1002/jbm.a.35813.
5. Ma B, Wang X, Wu C, Chang J. Crosslinking strategies for preparation of extracellular matrix-derived cardiovascular scaffolds. Regen Biomater. 2014;1:81–9. https://doi.org/10.1093/rb/rbu009.
6. Lin Y-C, Tan F-j, Marra KG, Jan S-S, Liu D-C. Synthesis and characterization of collagen/hyaluronan/chitosan composite sponges for potential biomedical applications. Acta Biomater. 2009;5:2591–600. https://doi.org/10.1016/j.actbio.2009.03.038.
7. Xu C, Lu W, Bian S, Liang J, Fan Y, Zhang X. Porous collagen scaffold reinforced with surfaced activated PLLA nanoparticles. Sci World J. 2012;2012:695137. https://doi.org/10.1100/2012/695137.
8. Chan EC, Kuo S-M, Kong AM, Morrison WA, Dusting GJ, Mitchell GM, et al. Three dimensional collagen scaffold promotes intrinsic vascularisation for tissue engineering applications. PLoS ONE. 2016;11:e0149799. https://doi.org/10.1371/journal.pone.0149799.
9. Ohyabu Y, Adegawa T, Yoshioka T, Ikoma T, Uemura T, Tanaka J. Cartilage regeneration using a porous scaffold, a collagen sponge incorporating a hydroxyapatite/chondroitinsulfate composite. Mater Sci Eng B. 2010;173:204–7. https://doi.org/10.1016/j.mseb.2009.12.008.
10. Liang W-H, Kienitz BL, Penick KJ, Welter JF, Zawodzinski TA, Baskaran H. Concentrated collagen-chondroitin sulfate scaffolds for tissue engineering applications. J Biomed Mater Res A. 2010;94:1050–60. https://doi.org/10.1002/jbm.a.32774.
11. Greene JJ, Sidle DM. The hyaluronic acid fillers: current understanding of the tissue device interface. Facial Plast Surg Clin North Am. 2015;23:423–32. https://doi.org/10.1016/j.fsc.2015.07.002.
12. Collins MN, Birkinshaw C. Hyaluronic acid-based scaffolds for tissue engineering—a review. Carbohydr Polym. 2013;92:1262–79. https://doi.org/10.1016/j.carbpol.2012.10.028.
13. Kreger ST, Voytik-Harbin SL. Hyaluronan concentration within a 3D collagen matrix modulates matrix viscoelasticity, but not fibroblast response. Matrix Biol. 2009;28:336–46. https://doi.org/10.1016/j.matbio.2009.05.001.
14. Murray MM, Spindler KP, Abreu E, Muller JA, Nedder A, Kelly M, et al. Collagen-platelet rich plasma hydrogel enhances primary repair of the porcine anterior cruciate ligament. J Orthop Res. 2007;25:81–91. https://doi.org/10.1002/jor.20282.
15. Hesse E, Hefferan TE, Tarara JE, Haasper C, Meller R, Krettek C, et al. Collagen type I hydrogel allows migration, proliferation and osteogenic differentiation of rat bone marrow stromal cells. J Biomed Mater Res A. 2010;94:442–9. https://doi.org/10.1002/jbm.a.32696.
16. He X, Kawazoe N, Chen G. Preparation of cylinder-shaped porous sponges of poly(L-lactic acid), poly(DL-lactic-co-glycolic acid), and poly(ε-caprolactone). Biomed Res Int. 2014;2014:106082. https://doi.org/10.1155/2014/106082.
17. Matuska AM, McFetridge PS. The effect of terminal sterilization on structural and biophysical properties of a decellularized collagen-based scaffold; implications for stem cell adhesion. J Biomed Mater Res B Appl Biomater. 2015;103:397–406. https://doi.org/10.1002/jbm.b.33213.
18. Noah EM, Chen J, Jiao X, Heschel I, Pallua N. Impact of sterilization on the porous design and cell behavior in collagen sponges prepared for tissue engineering. Biomaterials. 2002;23:2855–61.
19. Davidenko N, Schuster CF, Bax DV, Raynal N, Farndale RW, Best SM, et al. Control of crosslinking for tailoring collagen-based scaffolds stability and mechanics. Acta Biomater. 2015;25:131–42. https://doi.org/10.1016/j.actbio.2015.07.034.
20. Faraj KA, Brouwer KM, Geutjes PJ, Versteeg EM, Wismans RG, Deprest JA, et al. The effect of ethylene oxide sterilisation, beta irradiation and gamma irradiation on collagen fibril-based scaffolds. Tissue Eng Regen Med. 2011;8:460–70.
21. Awang MA, Firdaus MA, Busra MB, Chowdhury SR, Fadilah NR, Wan Hamirul WK, et al. Cytotoxic evaluation of biomechanically improved crosslinked ovine collagen on human dermal fibroblasts. Biomed Mater Eng. 2014;24:1715–24. https://doi.org/10.3233/BME-140983.
22. Ruijgrok JM, de Wijn JR, Boon ME. Glutaraldehyde crosslinking of collagen: Effects of time, temperature, concentration and presoaking as measured by shrinkage temperature. Clin Mater. 1994;17:23–7. https://doi.org/10.1016/0267-6605(94)90044-2.
23. McKegney M, Taggart I, Grant MH. The influence of crosslinking agents and diamines on the pore size, morphology and the biological stability of collagen sponges and their effect on cell penetration through the sponge matrix. J Mater Sci Mater Med. 2001;12:833–44.
24. Gough JE, Scotchford CA, Downes S. Cytotoxicity of glutaraldehyde crosslinked collagen/poly(vinyl alcohol) films is by the mechanism of apoptosis. J Biomed Mater Res. 2002;61:121–30. https://doi.org/10.1002/jbm.10145.

25. Ahmad Z, Shepherd JH, Shepherd DV, Ghose S, Kew SJ, Cameron RE, et al. Effect of 1-ethyl-3-(3-dimethylaminopropyl) carbodiimide and N-hydroxysuccinimide concentrations on the mechanical and biological characteristics of cross-linked collagen fibres for tendon repair. Regen Biomater. 2015;2:77–85. https://doi.org/10.1093/rb/rbv005.
26. Seto A, Gatt Jr. CJ, Dunn MG. Radioprotection of tendon tissue via crosslinking and free radical scavenging. Clin Orthop Relat Res. 2008;466:1788–95. https://doi.org/10.1007/s11999-008-0301-9.
27. Oloyede A, Broom ND. A physical model for the time-dependent deformation of articular cartilage. Connect Tissue Res. 1993;29:251–61.
28. Mow VC, Kuei SC, Lai WM, Armstrong CG. Biphasic creep and stress relaxation of articular cartilage in compression? Theory and experiments. J Biomech Eng. 1980;102:73–84.
29. Gibson LJ, Ashby MF. Cellular solids: structure and properties. The structure of cellular solids, Cambridge University Press, Cambridge, UK. 1999;43–7.
30. O'Brien FJ, Harley BA, Yannas IV, Gibson L. Influence of freezing rate on pore structure in freeze-dried collagen-GAG scaffolds. Biomaterials. 2004;25:1077–86.
31. Patel JM, Merriam AR, Culp BM, Gatt Jr. CJ, Dunn MG. One-year outcomes of total meniscus reconstruction using a novel fiber-reinforced scaffold in an ovine model. Am J Sports Med. 2016;44:898–907. https://doi.org/10.1177/0363546515624913.
32. Ran J, Hu Y, Le H, Chen Y, Zheng Z, Chen X, et al. Ectopic tissue engineered ligament with silk collagen scaffold for ACL regeneration: a preliminary study. Acta Biomater. 2017. https://doi.org/10.1016/j.actbio.2017.02.027.
33. Tamaddon M, Burrows M, Ferreira SA, Dazzi F, Apperley JF, Bradshaw A, et al. Monomeric, porous type II collagen scaffolds promote chondrogenic differentiation of human bone marrow mesenchymal stem cells in vitro. Sci Rep. 2017;7:43519. https://doi.org/10.1038/srep43519.
34. Powell HM, Boyce ST. EDC cross-linking improves skin substitute strength and stability. Biomaterials. 2006;27:5821–7. https://doi.org/10.1016/j.biomaterials.2006.07.030.
35. Mazor E, Zilberman M. Effect of gamma-irradiation sterilization on the physical and mechanical properties of a hybrid wound dressing. Polym Adv Technol. 2017;28:41–52. https://doi.org/10.1002/pat.3854.
36. Deyne PD, Haut RC. Some effects of gamma irradiation on patellar tendon allografts. Connect Tissue Res. 1991;27:51–62. https://doi.org/10.3109/03008209109006994.
37. Depalle B, Qin Z, Shefelbine SJ, Buehler MJ. Influence of cross-link structure, density and mechanical properties in the mesoscale deformation mechanisms of collagen fibrils. J Mech Behav Biomed Mater. 2015;52:1–13. https://doi.org/10.1016/j.jmbbm.2014.07.008.
38. Wang H-M, Chou Y-T, Wen Z-H, Wang Z-R, Chen C-H, Ho M-L. Novel biodegradable porous scaffold applied to skin regeneration. PLoS ONE. 2013;8:e56330. https://doi.org/10.1371/journal.pone.0056330.
39. Perez-Puyana V, Romero A, Guerrero A. Influence of collagen concentration and glutaraldehyde on collagen-based scaffold properties. J Biomed Mater Res A. 2016;104:1462–8. https://doi.org/10.1002/jbm.a.35671.
40. Tyan YC, Liao JD, Lin SP, Chen CC. The study of the sterilization effect of gamma ray irradiation of immobilized collagen polypropylene nonwoven fabric surfaces. J Biomed Mater Res A. 2003;67:1033–43. https://doi.org/10.1002/jbm.a.10024.